MINISTRY OF EDUCATION AND TRAINING

VIETNAM ACADEMY OF SCIENCE AND TECHNOLOGY

GRADUATE UNIVERSITY OF SCIENCE AND TECHNOLOGY

Vu Thanh Long

STATIC STABILITY OF FGM SHELLS WITH POROSITIES AND FG-CNTRC SANDWICH PANELS WITH ELASTICALLY RESTRAINED EDGES

Major: Engineering Mechanics

Code: 952 01 01

SUMMARY OF DISSERTATION ON MECHANICAL ENGINEERING AND ENGINEERING MECHANICS

Ha Noi, 2022

This work is completed at Graduate University of Science and Technology – Vietnam Academy of Science and Technology.

Scientific Supervisor 1: Associate Prof., Ph.D. Hoang Van Tung
Scientific Supervisor 2: Associate Prof., Ph.D. Dao Nhu Mai

Reviewer 1:
Reviewer 2:
Reviewer 3:

This dissertation will be upholden at Scientific Council of Graduate University of Sceince and Technology – Vietnam Academy of Science and Technology at …hour …. minutes, date …. month ……. year 2022

This dissertation can be found at the following places:
- Library of Graduate University of Science and Technology
- National Library of Vietnam

INTRODUCTION

1. The necessity of the dissertation

Functionally graded material (FGM) is an advanced composite possessing many superior properties such as very high stiffness and strength along with excellent temperature resistance. Therefreo, this composite is widely applied in many structural components. Nevertheless, in the manufacturing process, pores can exist within the FGM and have influences on the properties of the FGM. Accordingly, the effects of porosity on the static and dynamic responses in general and stability of FGM structures in particular are problems of great importance. Cylindrical, toroidal and spherical shells are extensively used in engineering and aerospace structures. However, the combined influences of porosity, elasticity of tangential edge constraints and transverse shear deformation on the linear and nonlinear instabilities of these shells have been not investigated.

Due to extremely high stiffness and strength along with very large aspect ratio, carbon nanotubes (CNTs) are ideal fillers into isotropic matrix to form carbon nanotube reinforced composite (CNTRC). Most of preceding works on the CNTRC structures only focused on single-layered form of CNTRC. There are very little investigations on the behavior of sandwich structures made of CNTRC. By virtue of the generation of new materials like CNTRC, the development of new sandwich models made of CNTRC is necessitated in order to optimize the performance of CNT-based structures. Flat and curved sandwich panels made of CNTRC have many superior characteristics and widely applied in micro and macro structures. Thus, the stability problem of CNTRC sandwich panels

must be considered. From above reasons and motivations, the dissertation aims to investigate *Stability of FGM shells with porosities and FG-CNTRC sandwich panels with elastically restrained edges*.

2. The aims of the dissertation

1) Linear buckling analysis of FGM cylindrical and toroidal shells with porosities and tangentially restrained edges. 2) Analysis of combined influences of porosities and elasticity of in-plane boundary conditions on the buckling and postbuckling behaviors of FGM circular plates, cylindrical and spherical shells subjected to mechanical, thermal and thermomechanical loads. 3) Nonlinear stability analysis of flat and curved sandwich panels made of FG-CNTRC including the elasticity of tangential constraints of edges.

3. Methodology

The dissertation uses the theoretical methodology based on analytical and semi-analytical approaches. Governing equations are established based on the classical shell theory (CST), first-order shear deformation theory (FSDT) and higher-order shear deformation theory (HSDT), then are solved using Galerkin method and iteration.

4. The main content of the dissertation

The dissertation includes 5 chapters. Chapter 1 reviews the previous publications. Chapter 2 studies linear stability of FGM cylindrical and toroidal shells with porosities. Nonlinear stability of FGM cylindrical shells with porosities is presented in chapter 3 using FSDT. Chapter 4 analyzes nonlinear stabilities of porous FGM spherical shells and circular plates. Finally, buckling and postbuckling of FG-CNTRC sandwich panels are investigated in chapter 5.

CHAPTER 1. REVIEW

In the first part of this chapter, the dissertation has reviewed the functionally graded material (FGM), and superior properties of carbon nanotubes (CNTs) and functionally graded carbon nanotube reinforced composite (FG-CNTRC). In the next part of chapter 1, the preceding works on the stability problem of FGM shells and single-layered and sandwich FG-CNTRC structures have been reviewed. Specifically, the dissertation reviewed previous studies on the linear and nonlinear instabilities of FGM cylindrical and toroidal shells without porosities; on the stability of FGM shallow spherical shells and circular plates without porosities; on the behavior of FGM structures with porosities; on the stability of single-layered and sandwich FG-CNTRC structures. From the review, it is remarked that:

- There are little publications on the stability of FGM structures with porosities. Especially, there are no investigations on the linear and nonlinear stabilities of porous FGM cylindrical and toroidal shells.

- Nonlinear stability of FGM spherical shells and circular plates with porosities and restrained edges have been not investigated.

- Among previous studies on FG-CNTRC sandwich structures, only sandwich model with homogeneous core and FG-CNTRC face sheets was considered. Another sandwich model composed of FG-CNTRC core and homogeneous face sheets have been not considered.

- There are no studies examining the combined influences of porosity and edge constraints on the stability of shear deformable FGM closed shells, FGM spherical shells and circular plates.

- There is a very limited number of preceding works considering the effects of three-parameter nonlinear foundations on the behavior of composite structures and particularly stability of FGM structures.

The dissertation focuses to deal with the above problems.

CHAPTER 2. LINEAR BUCKLING OF FGM TOROIDAL SHELL SEGMENTS WITH POROSITIES USING HIGHER ORDER SHEAR DEFORMATION THEORY

2.1. Material and structural models

Structural model considered in this chapter is a toroidal shell segment (TSS) shown in Fig. 2.1. The TSS is surrounded by an elastic medium, exposed to a thermal environment $\Delta T = T - T_0$ and subjected to axial compression P, lateral pressure q or combined action of mechanical loads P and q.

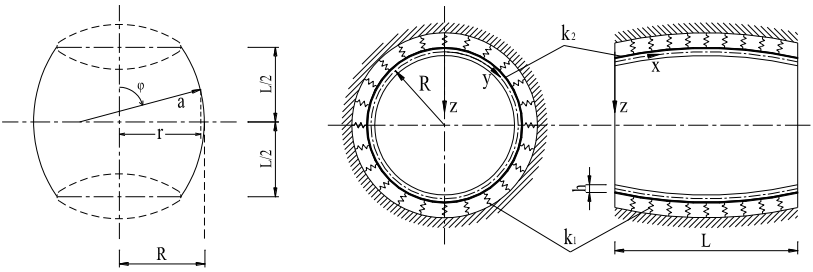

Figure 2.1. Geometry and coordinates of a toroidal shell segment.

The dissertation accounts for elasticity of in-plane constraints of edges. Specifically, two edges are elastically modelled as Fig. 2.2.

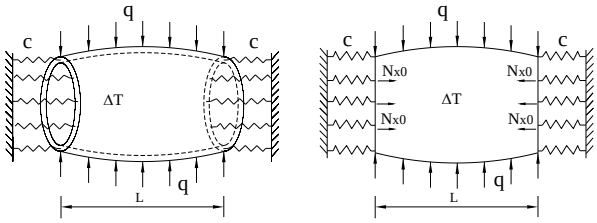

Figure 2.2. Model of tangentially elastic constraints of boundary edges.

The TSS is made of FGM with porosities, in which pores are distributed within FGM according to even and uneven distributions, as illustrated in Fig. 2.3.

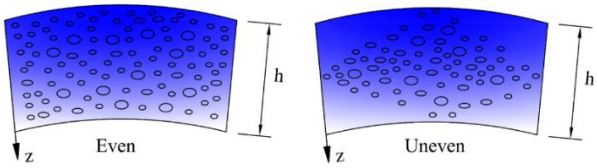

Figure 2.3. Illustrations of even and uneven types of porosity distribution.

Due to the existence of pores, the effective properties P_{eff} of FGM can be determined using a modified rule of mixture as.

$$P_{eff} = P_m\left(V_m - \frac{\xi}{2}\right) + P_c\left(V_c - \frac{\xi}{2}\right) \tag{2.1}$$

in which $0 \le \xi \ll 1$ is porosity volume fraction and $\xi = 0$ for perfect FGM (i.e. without porosity). Effective modul of elasticity E and coefficient of thermal expansion α of FGM with porosities are

$$E(z,T) = \left[E_m(T) - E_c(T)\right]\left(\frac{1}{2} + \frac{z}{h}\right)^N + E_c - \frac{\xi}{2}\left[E_m(T) + E_c(T)\right]\left(1 - 2\tau\frac{|z|}{h}\right) \tag{2.2a}$$

$$\alpha(z,T) = \left[\alpha_m(T) - \alpha_c(T)\right]\left(\frac{1}{2} + \frac{z}{h}\right)^N + \alpha_c - \frac{\xi}{2}\left[\alpha_m(T) + \alpha_c(T)\right]\left(1 - 2\tau\frac{|z|}{h}\right) \tag{2.2b}$$

where $\tau = 0$ and $\tau = 1$ for even and uneven distributions, respectively.

2.2. Governing equations and analytical solutions

Governing equations including the equilibrium equation and strain compatibility equation are established within the framework of higher order shear deformation theory (HSDT) in terms of deflection function w, stress function f and rotations ϕ_x, ϕ_y. Specifically, the equilibrium equation is derived as follows:

$$c_1^2\left(\frac{D_2D_5}{D_4} - D_3\right)\nabla^6 w + \left(c_1\frac{D_2}{D_4} + 1\right)D_6\nabla^4 w$$
$$+\left(1 - c_1\frac{D_5}{D_4}\right)\nabla^2\left(f_{,yy}w_{,xx} - 2f_{,xy}w_{,xy} + f_{,xx}w_{,yy} + \frac{f_{,yy}}{a} + \frac{f_{,xx}}{R} + q - k_1w + k_2\nabla^2 w\right)$$
$$-\frac{D_6}{D_4}\left(f_{,yy}w_{,xx} - 2f_{,xy}w_{,xy} + f_{,xx}w_{,yy} + \frac{f_{,yy}}{a} + \frac{f_{,xx}}{R} + q - k_1w + k_2\nabla^2 w\right) = 0 \tag{2.3}$$

where $\nabla^2 = \partial^2 / \partial x^2 + \partial^2 / \partial y^2$ is Laplace operator. Strain compatibility equation is written in the form

$$\nabla^4 f + E_1 \left(\frac{w_{,xx}}{R} + \frac{w_{,yy}}{a} \right) = 0 . \tag{2.4}$$

Fictitious force N_{x0} at restrained edges and closed condition:

$$N_{x0} = -\frac{c}{2\pi RL} \int_0^{2\pi R} \int_0^{L} \frac{\partial u}{\partial x} dxdy \ , \ \int_0^{2\pi R} \int_0^{L} \frac{\partial v}{\partial y} dxdy = 0 \tag{2.5a,b}$$

To satisfy simply supported conditions of edges, approximate analytical solutions are assumed as the following

$$w(x,y) = W_0 + W_1 \sin \beta_m x \sin \delta_n y$$

$$f(x,y) = A_1 \cos 2\beta_m x + A_2 \cos 2\delta_n y + A_3 \sin \beta_m x \sin \delta_n y - \frac{1}{2}\sigma_{0y} h x^2 + \frac{1}{2} N_{x0} y^2$$

$$\phi_x = B_1 \cos \beta_m x \sin \delta_n y \ , \ \phi_y = B_2 \sin \beta_m x \cos \delta_n y \tag{2.6}$$

Using (2.6) into equilibrium equation and applying Galerkin method

$$-\bar{N}_{x0} \frac{R_a}{R_h} + \frac{\sigma_{0y}}{R_h} - q + K_1 \frac{E_m^0}{R_h^4} \bar{W}_0 = 0 \tag{2.7a}$$

$$\frac{1 + a_{11}}{R_h^2} \left(\bar{N}_{x0} \frac{m^2 \pi^2}{L_R^2} - \sigma_{0y} n^2 \right) + a_{21} = 0 \tag{2.7b}$$

2.3. Specific problems

2.3.1. TSS with restrained edges under lateral load and temperature.

By determining N_{x0} and σ_{0y} from conditions (2.5a,b), substituting into (2.7) and eleminating $\bar{W}_0$ from the resulting equations, we obtain buckling lateral pressure q of porous TSS as

$$q = g_{11} g_{12} - \left(g_{11} g_{22} - g_{21} \right) \Delta T \tag{2.8}$$

2.3.2. TSS with movable edges under combined mechanical loads

TSS with movable edges under combined action of axial pressure P at edges and lateral pressure q. Determining σ_{0y} from (2.5b) and putting σ_{0y} and $\bar{N}_{x0} = -P$ into (2.7) and the eleminating $\bar{W}_0$ yields

$$P = \frac{a_{22} - a_{32}\Delta T}{\gamma + a_{12}} \tag{2.9}$$

where $\gamma = q/P$ is load ratio. Critical loads P_{cr} , q_{cr} , ΔT_{cr} are the smallest values of buckling loads with respect to buckling mode (m, n).

2.4. Numerical results and discussion

This section presents some numerical results for buckling analysis of FGM TSSs made of two material constituents are that silicon nitride (Si_3N_4) and stainless steel ($SUS304$) properties of which are assumed to be temperature dependent.

To verify the proposed approach, a comparative study is carried out for critical loads of perfect FGM cylindrical shells with movable edges under combined mechanical loads. Critical loads obtained by using Eq. (2.9) are shown in Table 2.3 in comparison with results reported in the work of Shen and Noda [30] using asymptotic solutions. It is evident that a good agreement is achieved in this comparison.

Table 2.3. Comparision of critical loads (P_{cr}, q_{cr})(MPa) of FGM cylindrical shells under combined mechanical load ($R/h = 30$, $L^2/Rh = 500$, $\Delta T = 0$ K).

N	source	(P_{cr}, q_{cr}) (MPa)			
0.2	Ref. [30]	(4110.57, 0)	(3865.17, 2.577)	(1248.38, 8.323)	(0, 11.061)
	Present	(4510.5, 0) *	(3865.17, 2.578)	(1248.377, 8.323)	(0, 11.061)
1.0	Ref. [30]	(4735.33, 0)	(4420.00, 2.947)	(1427.56, 9.571)	(0, 12.648)
	Present	(5192.4, 0)	(4420.00, 2.949)	(1427.56, 9.530)	(0, 12.648)
2.0	Ref. [30]	(5018.19, 0)	(4654.40, 3.103)	(1503.25, 10.022)	(0, 13.319)
	Present	(5499.1, 0)	(4654.40, 3.105)	(1503.25, 10.022)	(0, 13.319)

* Mode $(m,n) = (13,1)$ with $q_{cr} = 0$ and $(m,n) = (1,3)$ with others.

Effects of Gauss curvature R/a , porosity volume fraction ξ and non-dimensional stiffness K_1, K_2 of foundation on critical loads

q_{cr} of FGM TSS with evenly distributed porosities and immovable edges ($\lambda = 1$) under lateral pressure are shown in Fig. 2.4. Obviously, q_{cr} are significantly decreased and increased when ξ and R/a is increased, respectively. Additionally, q_{cr} is larger as enhancing K_1, K_2.

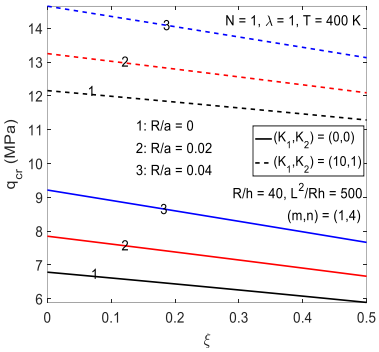

Figure 2.4. Effects R/a, ξ and K_1, K_2 on critical lateral pressure q_{cr} of FGM TSSs.

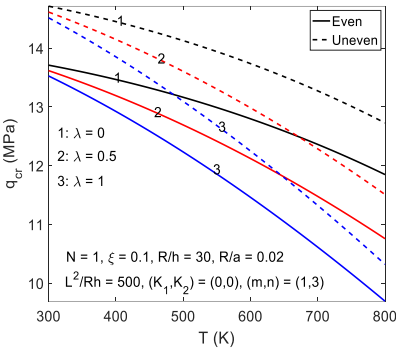

Figure 2.5. Effects of temperature, edge restraint λ and porosity distribution on q_{cr}.

Figure 2.5 indicates that critical pressure q_{cr} is slightly and strongly reduced when edges are more severely restrained (higher λ) at reference and elevate temperatures, and q_{cr} is lower for even type.

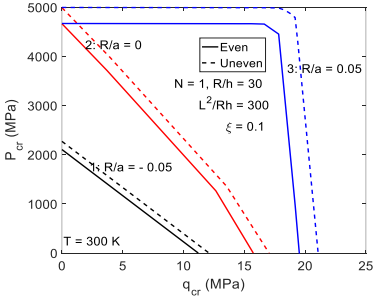

Figure 2.6. Effects of R/a and porosity distribution on the stability region of FGM TSS.

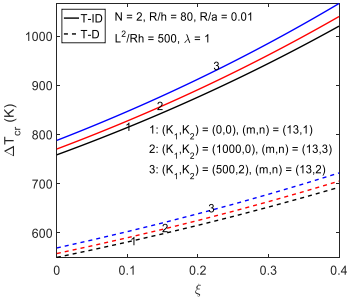

Figure 2.7. Effect of porosity volume fraction on critical temperature ΔT_{cr} of FGM TSS.

Next, Fig. 2.6 examines effects of Gauss curvature R/a and porosity distribution on the stability region of FGM TSSs under combined mechanical loads. Obviously, the stability region of cylindrical shell ($R/a = 0$) is larger and remarkably smaller than those of concave ($R/a < 0$) and convex ($R/a > 0$) TSSs, respectively, and is more narrow for even distribution. Finally, Fig. 2.7 indicates the effects of porosity volume fraction ξ on critical thermal loads ΔT_{cr} of FGM TSSs under uniform temperature rise. Evidently, unlike case of mechanical loads, porosities have beneficial influences on buckling resistance of TSS and critical temperature ΔT_{cr} is larger for higher ξ .

2.5. Conclusions of chapter 2

1. Porosities have beneficial and deteriorative influences on the stability of FGM shells under thermal and mechanical loads, respectively.

2. Critical thermal loads are higher when pores are evenly distributed in the FGM. In contrast, critical mechanical loads are larger as pores are unevenly distributed in the FGM.

3. Critical loads are considerably enhanced when shells are surrounded by an elastic medium. Winkler-type foundation more beneficially influences the FGM TSS under lateral pressure.

4. Critical pressures of TSSs are slightly and significantly reduced when edges are restrained at reference and elevated temperatures.

5. When the TSS is exposed to uniform temperature, critical temperature is strongly decreased as edges are more rigorously restrained and/or preexistent lateral pressure is enhanced.

Main results of chapter 2 have been presented in 2 scientific papers published on international journals ranking ISI, that is, papers numbered 1 and 2 in the list of author's scientific works relating to the content of the dissertation.

CHAPTER 3. NONLINEAR STABILITY OF FGM CIRCULAR CYLINDRICAL SHELLS WITH POROSITIES USING FSDT

3.1. Material and structural models

This chapter considers a geometrically perfect circular cylindrical shell (CCS) of length L, radius R and thickness h, as shown in Fig. 3.1.

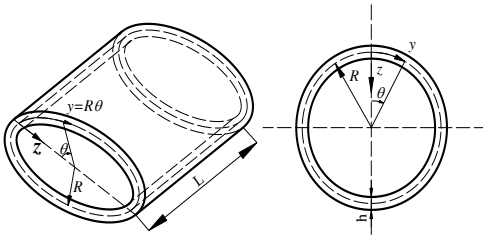

Figure 3.1. Geometry of cylindrical shell.

Two boundary edges $x = 0, L$ of cylindrical shell are simply supported and tangentially restrained as illustrated in chapter 2. The shell is made of FGM with porosities the effective properties of which are expressed as section 2.1 in the chapter 2.

3.2. Governing equations and analytical solution

In the present chapter, the first order shear deformation theory (FSDT) is used to establish governing equations for the nonlinear stability problem of FGM cylindrical shells with porosities under mechanical and thermal loads. Specifically, nonlinear equilibrium equation and strain compatibility equation are written in terms of deflection w, stress function f, and rotations ϕ_x, ϕ_y. The nonlinear equilibrium equation basing on the FSDT has the form

$$D\nabla^2\left(\phi_{x,x} + \phi_{y,y}\right) + f_{,yy}w_{,xx} - 2f_{,xy}w_{,xy} + f_{,xx}w_{,yy} + f_{,xx}/R + q = 0 \quad (3.1)$$

Strain compatibility equation is written in the form:

$$\nabla^4 f + E_1\left(\frac{w_{,xx}}{R} + w_{,xx}w_{,yy} - w_{,xy}^2\right) = 0 \quad (3.2)$$

Approximate analytical solutions are assumed as Eq. (2.6).

By placing the solutions (2.6) into compatibility equation (3.2), coefficients A_1, A_2, A_3 can be determined. Substituting solutions (2.6) into equilibrium equation (3.1) and applying Galerkin method give

$$-\frac{\sigma_{0y}}{R_h} + q = 0 \tag{3.3a}$$

$$-g_{11} - g_{21}\bar{W}_1^2 - \frac{m^2\pi^2}{R_h^2 L_R^2}\bar{N}_{x0} + \frac{n^2}{R_h^2}\sigma_{0y} = 0 \tag{3.3b}$$

where g_{11}, g_{21} are quantities depending on material and geometry properties, $R_h = R/h$, $L_R = L/R$ and q is external lateral pressure.

3.3. Specific problems

3.3.1. *CCS with restrained edges under pressure and temperature*

From kinematic relations and expressions of resultant forces, $u_{,x}, v_{,y}$ are expressed in terms of partial derivative of f, w, ϕ_x, ϕ_y. Afterwards, by putting $u_{,x}, v_{,y}$ into relations (2.5a,b), we obtain a system of two algebraic equations from which fictitious force resultant $\bar{N}_{x0}$ and circumferential stress σ_{0y} are determined as follows

$$\bar{N}_{x0} = -g_{13}\bar{W}_0 + g_{23}\bar{W}_1^2 - g_{33}\Delta T,\ \sigma_{0y} = g_{12}\bar{W}_0 - g_{22}\bar{W}_1^2 + g_{32}\Delta T \tag{3.4}$$

Substituting (3.4) into (3.3) and eleminating $\bar{W}_0$ from resulting equations lead to the following relation between load and deflection

$$q = \frac{1}{g_{14}}\left(g_{11} + g_{24}\bar{W}_1^2 - g_{34}\Delta T\right) \tag{3.5}$$

Non-dimensional maximum deflection is written in the form

$$\bar{W}_{\max} = \bar{W}_0 + \bar{W}_1 = \bar{W}_1 + \frac{g_{22}}{g_{12}}\bar{W}_1^2 - \frac{g_{32}}{g_{12}}\Delta T + \frac{R_h}{g_{12}}q \tag{3.6}$$

Expressions (3.5) and (3.6) are used to determine load-deflection curves for postbuckling analysis of porous FGM CCS under lateral pressure in thermal environments. Buckling lateral pressure is obtained from Eq. (3.5) by setting $\bar{W}_1 = 0$ as the following

$$q_b = \frac{1}{g_{14}}\left(g_{11} - g_{34}\Delta T\right) \tag{3.7}$$

When CCS is only exposed to uniform temperature rise, relation between thermal load ΔT and deflection and buckling load ΔT_b can be obtained from (3.5) and (3.7) as $q = 0$, but omitted here for brevity.

3.3.2. CCS with movable edges under combined mechanical loads

By determining σ_{0y} from (2.5b), putting $\bar{N}_{x0} = -P$ and σ_{0y} into (3.3) and eleminating $\bar{W}_0$ from resulting equations, we obtain

$$P = \frac{R_h^2 L_R^2}{m^2\pi^2 + \gamma n^2 R_h L_R^2}\left(g_{11} + g_{21}\bar{W}_1^2\right) \tag{3.8}$$

in which $\gamma = q / P$ is load ratio.

3.4. Numerical results and discussion

This section presents numerical results for postbuckling analysis of FGM CCSs made of Si_3N_4 and $SUS304$ with porosities.

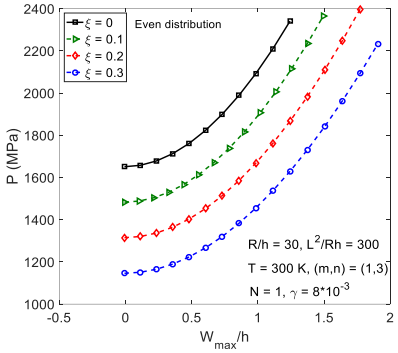

Figure 3.2. Effects of porosity volume fraction ξ on the postbuckling of CCS.

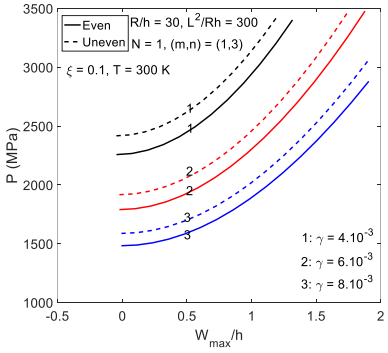

Figure 3.3. Postbuckling of FGM CCS with various load ratios and porosity distributions.

Figure 3.2 indicates that load capacity of CCS is strongly reduced when ξ is increased. Figure 3.3 demonstrates that increase in

preexistent external pressure makes load carrying capability of axially loaded CCSs is significantly lowered.

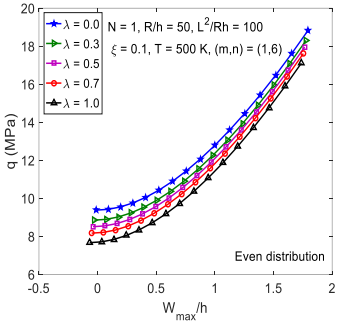

Figure 3.4. Effects of λ on postbuckling of CCS under q.

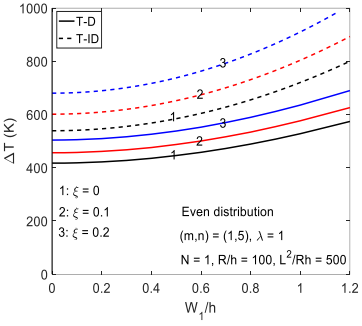

Figure 3.5. Effects of ξ on postbuckling of CCS under T.

Fig. 3.4 shows that pressure carrying of CCS is considerably decreased as edges are restrained at elevated temperature. Figure 3.5 indicates beneficial influences of porosity on thermal stability of CCS.

3.5. Conclusions of chapter 3.

1. Porosities have negative and positive influences on the mechanical and thermal stabilities of FGM CCSs, respectively.

2. Lateral pressure capacity of CCS is slightly and considerably reduced as edges are restrained at reference and elevated temperatures.

3. Influence of porosity distribution depends on type of loading, porosity volume fraction and volume fraction index (N).

4. Pre-existent temperature has detrimental effect on the mechanical stability of CCS. Nevertheless, negative influence of T is slightly lowered as porosity percentage in the FGM is increased.

Main results of chapter 3 have been presented in 2 papers published on international scientific journals ranking ISI, that are papers numbered 3 and 4 in the list of author's scientific works relating to the content of the dissertation.

CHAPTER 4. NONLINEAR STABILITY OF FGM SPHERICAL CAPS AND CIRCULAR PLATES WITH POROSITIES AND ELASTICALLY RESTRAINED EDGES

4.1. Material and structural models

This chapter considers FGM spherical caps of curvature radius R, base radius a, thickness h and rise H,as shown in Fig 4.1

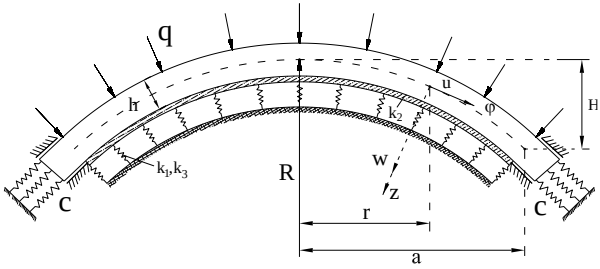

Figure 4.1. Spherical cap under external pressure.

Spherical cap (SC) is assumed to be very shallow ($H \ll a$), rested on a three-parameter nonlinear elastic foundation and subjected to uniform external pressure q .Boundary edge is clamped and elastically restrained in the meridional direction. SC is made of porous FGM with poroperties as chapter 2 and under axisymmetric deformation.

4.2. Governing equations and analytical solution

In the present chapter the SC is assumed to be thin and geometrically imperfect. Nonliear equilibrium equation and strain compatibility equation in terms of deflection w and stress function f are established within the framework of the classical shell theory (CST). Due to axisymmetric deformation assumption, basic equations only depend on meridional coordinate variable φ . In the establishment of the governing equations, for the purpose of mathematical convenience and simplicity, meridional coordinate φ is replaced by radius of meridional circle $r = R\sin\varphi$ (Fig. 4.1). Specifically, nonlinear equilibrium equation is written as

$$D\Delta_s^2 w-\frac{1}{R}\Delta_s f-\frac{1}{r}f'\left(w+w^*\right)''-\frac{1}{r}f''\left(w+w^*\right)'-q+k_1 w-k_2\Delta_s w+k_3 w^3=0 \tag{4.1}$$

where, in this chapter, superscript comma indicates derivative with respect to variable r (e.g. $f'=df/dr$), $\Delta_s()=()''+()'/r$ is Laplace operator in the case of axisymmetric deformation, w^* is initial geometrical imperfection, q is external pressure, while k_1, k_2 and k_3 are stiffness paramters of Winkler elastic layer, Pasternak shear layer and nonlinear Winkler foundation. Compatibility equation is written:

$$\frac{1}{E_1}\Delta_s^2 f=-\frac{1}{R}\Delta_s w-\frac{1}{r}\left(\frac{dw}{dr}\frac{d^2w}{dr^2}+\frac{dw^*}{dr}\frac{d^2w}{dr^2}+\frac{dw}{dr}\frac{d^2w^*}{dr^2}\right) \tag{4.2}$$

Boundary condition and symmetry condition at apex are

$$w=W\ ,\ w'=0\ ,\ N_r\ \text{ is finite at apex }\ r=0 \tag{4.3a}$$

$$w=0\ ,\ w'=0\ ,\ \ N_r=N_{r0}\qquad \text{at edge}\ \ r=a \tag{4.3b}$$

where W is amplitude of deflection (at apex) and N_{r0} is fictitious force at edge related to Δ_r and tangential stiffness c as follows

$$N_{r0}=c\Delta_r\ ,\ \Delta_r=-\frac{1}{2a}\int_{-a}^{a}\frac{du}{dr}dr \tag{4.4}$$

Approximate analytical solution of deflection is chosen as

$$w=\frac{W}{a^4}\left(a^2-r^2\right)^2\ ,\ w^*=\frac{\mu h}{a^4}\left(a^2-r^2\right)^2 \tag{4.5}$$

Placing (4.5) into compatibility equation (4.2) and integrating the obtained equation, integration constants are determined using condition of finiteness of N_r at $r=0$ and $N_r(r=a)=N_{r0}$, we receive

$$\frac{df}{dr}=-\frac{E_1}{6a^4R}\left(r^5-3a^2r^3\right)W-\frac{E_1}{6a^8}\left(r^7-4a^2r^5+6a^4r^3\right)W\left(W+2\mu h\right)$$
$$+\frac{E_1 r}{2a^2}W\left(W+2\mu h\right)-\frac{E_1 r}{3R}W+N_{r0}r \tag{4.6}$$

Using deflection solution (4.5) and stress function (4.6) into equilibrium equation (4.1) and applying Galerkin method lead to

$$q=\bar{g}_{11}\overline{W}-\bar{g}_{21}\overline{W}\left(\overline{W}+\mu\right)-\bar{g}_{31}\overline{W}\left(\overline{W}+2\mu\right)+\bar{g}_{41}\overline{W}\left(\overline{W}+\mu\right)\left(\overline{W}+2\mu\right)$$
$$+\bar{g}_{51}\overline{W}^{3}-\bar{g}_{61}\left[\frac{2}{R_h R_a^2}\left(\overline{W}+\mu\right)-1\right]\Delta T \qquad (4.7)$$

Expression (4.7) is nonlinear relation between load and deflection of porous FGM spherical cap exposed to a thermal environment, rested on an elastic foundation and subjected to external pressure. Specialization of (4.7) for the case of $q=0$ and $R\to\infty$ yield

$$\Delta T=\frac{\bar{E}_1+\bar{c}(1-\nu)}{4\bar{c}G\beta^2}\left(64\bar{D}+\frac{3}{5}E_m^0K_1+4E_m^0K_2\right)\frac{\overline{W}}{\overline{W}+\mu} \qquad (4.8)$$
$$+\frac{\bar{E}_1}{14\bar{c}G\beta^2}\left[3\bar{E}_1+\bar{c}\left(\frac{23}{3}-3\nu\right)\right]\overline{W}\left(\overline{W}+2\mu\right)+\frac{E_m^0K_3\left[\bar{E}_1+\bar{c}(1-\nu)\right]}{12\bar{c}G\beta^4}\frac{\overline{W}^3}{\overline{W}+\mu}$$

This is nonlinear relation between thermal load and deflection of porous FGM circular plate on elastic foundation under temperature.

4.3. Numerical results

After performing comparative studies to verify accuracy of the proposed approach, some major results are presented in the following.

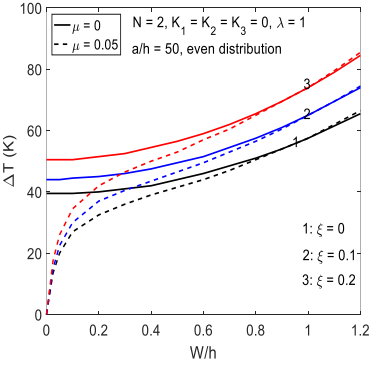

Fig 4.2. Effects of porosity percentage on postbuckling of FGM circular plate under T.

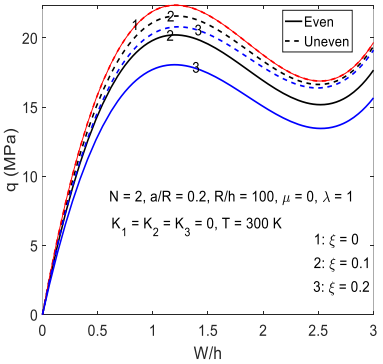

Fig. 4.3. Effects of porosity percentage on postbuckling of FGM SC under external pressure.

Fig. 4.2 indicates positive influence of porosity on the stability of FGM circular plate under temperature. In contrast, Fig. 4.3 shows that porosity negatively influence stability of SC undergoing pressure.

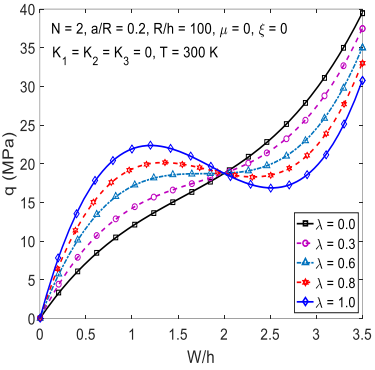

Figure 4.4. Effect of edge constraint on the postbuckling of porous SC under pressure.

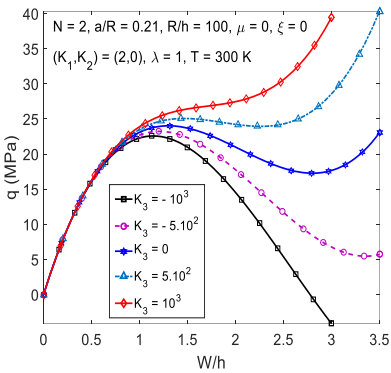

Figure 4.5. Effect of nonlinear foundation on stability of porus SC under external pressure.

4.4. Conclusions of chapter 4.

1. Porosities have positive and negative influences on stabilities of thermally loaded plates and pressure-loaded SC, respectively.

2. Tangential edge constraint reduces critical load and postbuckling strength of thermally loaded circular plate. In contrast, edge constraint enhances both critical pressure and snapping jump of pressure-loaded FGM SCs.

3. Pressure-loaded FGM SCs exhibit a bifurcation-quasi buckling response due to edge constraint and pre-existent temperature.

4. Elastic foundation has positive influences on the nonlinear stability of pressure-loaded SCs. Snapping jumps can be alleviated or eliminated when SC is supported by nonlinear elastic foundation.

Main results of chapter 4 have been presented in 1 scientific paper published on international journal ranking ISI, that is paper numbered 5 in the list of author's scientific works relating to the content of the dissertation.

CHAPTER 5. NONLINEAR STABILITY OF FG-CNTRC SANDWICH PLATES AND PANELS WITH ELASTICALLY RESTRAINED EDGES

5.1. Material and structural models

Considered in this chapter are sandwich panels in the doubly curved, cylindrical or flat geometries of total thickness h, plan-form dimensions a,b and curvature radii R_x, R_y.

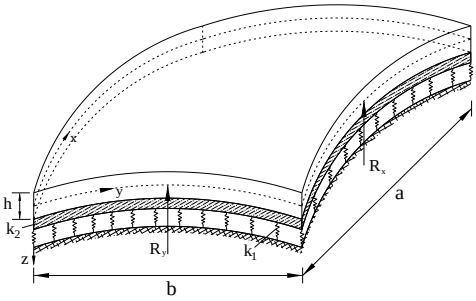

Figure 5.1. Doubly curved panel

Cylindrical panel is case as $R_x \to \infty$, $R_y = R$ and flat panel (i.e. plate) is received as $R_x \to \infty, R_y \to \infty$. Two sandwich models studied:

Sandwich model of type A consists of homogeneous core and two face sheets made of FG-CNTRC, as illustrated in Figure 5.2.

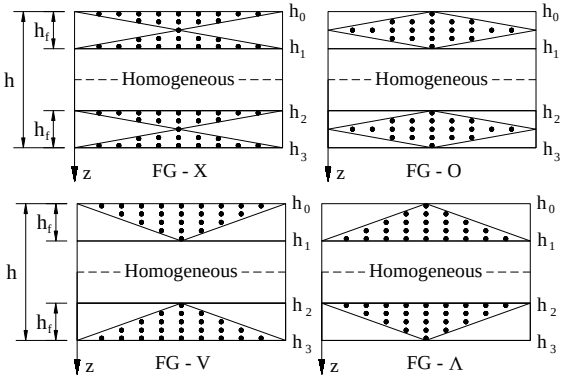

Figure 5.2. FG distributions of CNTs in sandwich model of type A.

Sandwich model of type B consists of FG-CNTRC core and two homogeneous face sheets, as sketched in Figure 5.3.

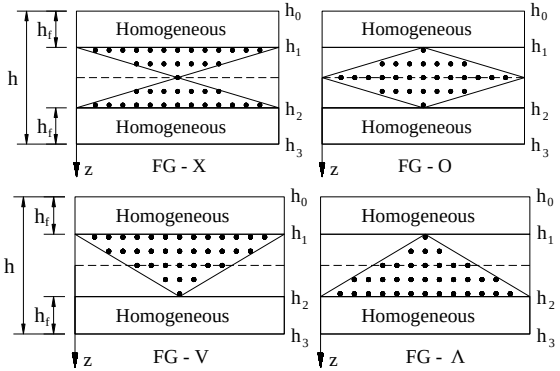

Figure 5.3. FG distributions of CNTs in sandwich model of type B.

Effective elastic moduli and shear modulus of FG-CNTRC layer are determined using an extended rule of mixture as follows

$$E_{11} = \eta_1 V_{CNT} E_{11}^{CNT} + V_m E^m \tag{5.1a}$$

$$\frac{\eta_2}{E_{22}} = \frac{V_{CNT}}{E_{22}^{CNT}} + \frac{V_m}{E^m} \tag{5.1b}$$

$$\frac{\eta_3}{G_{12}} = \frac{V_{CNT}}{G_{12}^{CNT}} + \frac{V_m}{G^m} \tag{5.1c}$$

5.2. Governing equations and analytical solution

Nonlinear equilibrium equation and strain compatibility equation are derived based on the first order shear deformation theory (FSDT) are expressed in terms of deflection w, stress function f and rotations ϕ_x, ϕ_y. Equilibrium equation is expressed in the form as

$$a_{11}\phi_{x,xxx} + a_{21}\phi_{x,xyy} + a_{31}\phi_{y,xxy} + a_{41}\phi_{y,yyy} + a_{51} f_{,xxyy} + f_{,yy}\left(w_{,xx} + w^*_{,xx}\right) \tag{5.2}$$

$$-2 f_{,xy}\left(w_{,xy} + w^*_{,xy}\right) + f_{,xx}\left(w_{,yy} + w^*_{,yy}\right) + \frac{f_{,yy}}{R_x} + \frac{f_{,xx}}{R_y} + q - k_1 w + k_2\left(w_{,xx} + w_{,yy}\right) = 0$$

Strain compatibility equation is written in the form

$$a_{12} f_{,xxxx} + a_{22} f_{,xxyy} + a_{32} f_{,yyyy} + a_{42}\phi_{x,xxx} + a_{52}\phi_{y,xxy} + a_{62}\phi_{y,yyy} + a_{72}\phi_{x,xyy}$$

$$-w^2_{,xy} + w_{,xx} w_{,yy} - 2 w_{,xy} w^*_{,xy} + w_{,xx} w^*_{,yy} + w_{,yy} w^*_{,xx} + \frac{w_{,yy}}{R_x} + \frac{w_{,xx}}{R_y} = 0 \tag{5.3}$$

Analytical solution satisfying simply supported edges conditions

$$\left(w, w^*\right) = \left(W, \mu h\right) \sin \beta_m x \sin \delta_n y$$

$$f = A_1 \cos 2\beta_m x + A_2 \cos 2\delta_n y + A_3 \sin \beta_m x \sin \delta_n y + \frac{1}{2} N_{x0} y^2 + \frac{1}{2} N_{y0} x^2$$

$$\phi_x = B_1 \cos \beta_m x \sin \delta_n y \ , \ \phi_y = B_2 \sin \beta_m x \cos \delta_n y \qquad (5.4)$$

Applying Galerkin method yields the following relation

$$a_{13}\overline{W} + a_{23}\overline{W}\left(\overline{W} + \mu\right) + a_{33}\overline{W}\left(\overline{W} + 2\mu\right) + a_{43}\overline{W}\left(\overline{W} + \mu\right)\left(\overline{W} + 2\mu\right) - \frac{16q}{mn\pi^2}\gamma_m\gamma_n$$

$$+\left(\bar{N}_{x0} m^2 B_a^2 + \bar{N}_{y0} n^2\right)\frac{\pi^2}{B_h^2}\left(\overline{W} + \mu\right) - \left(\bar{N}_{x0} B_a R_1 + \bar{N}_{y0} R_2\right)\frac{16}{mn\pi^2 B_h}\gamma_m\gamma_n = 0 \qquad (5.5)$$

From general relation (5.5), nonlinear load–deflection relations for the following problems are formulated 1) Doubly curved panel with elastically restrained edges under external pressure in thermal environments, 2) Cylindrical panel with movable edges subjected to axial compression in thermal environments, 3) Rectangular plate with tangentially restrained edges under uniform temperature rise, and 4) Rectangular plate with movable edges $x = 0, a$ and tangentially restrained edges $y = 0, b$ undergoing the combined action of compression in movable edges and uniform temperature rise.

5.3. Numerical results

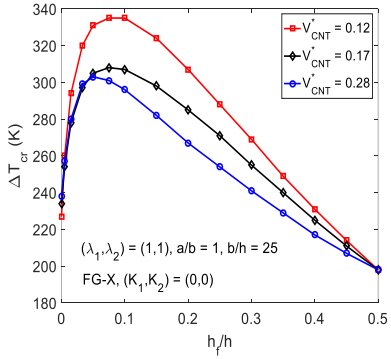

Figure 5.4. Critical thermal loads of sandwich plate type B.

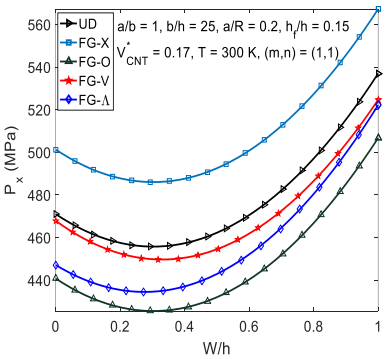

Figure 5.5. Postbuckling of sandwich cylindrical panel.

Fig. 5.4 indicates that there exists an optimal ratio of thicknesses of layers for which the critical thermal load of sandwich plate of type B is the highest. Fig. 5.5 demonstrates that FG-X distribution makes the compressive load capacity of cylindrical panels of type B strongest.

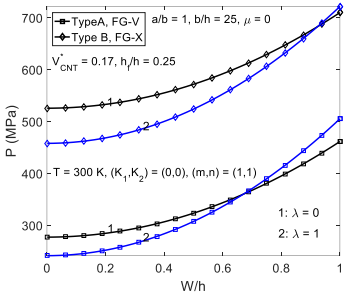

Figure 5.6. The postbuckling behavior of sandwich plates of types A & B under compression.

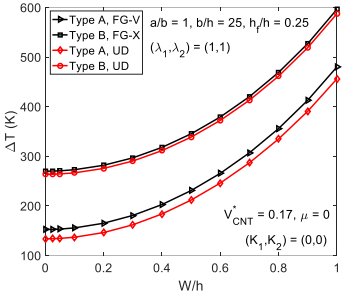

Figure 5.7. The postbuckling behavior of sandwich plates of types A & B under temperature.

Comparisons shown in Figures 5.6 and 5.7 indicate that, with the same volume fraction of material constituents, sandwich model of type B with homogeneous face sheets and FG-CNTRC core bring to much stronger loading capacity than that of sandwich model of type A.

5.4. Conclusions of chapter 5

1. Postbuckling strength of curved sandwich panels under external pressure and sandwich plates undergoing thermal load are increased and decreased when edges are more restrained, respectively.

2. When sandwich plate is exposed to a thermal environment, a small percentage of CNT in FG-CNTRC layer gives the best stablility.

3. Sandwich model of type B with FG-CNTRC core and homogeneous face sheets has many advanced properties and potential applications in practical structures.

Major results of chapter 5 have been presented in 4 scientific papers including 2 papers published on international journal ranking ISI and 2 papers published on Vietnam Journal of Mechanics, that are papers numbered 6,7,8 and 9 in the list of author's scientific works relating to the content of the dissertation.

CONCLUSIONS

The dissertation has obtained some new results as the following:

1. The dissertation has analyzed the linear buckling of thick FGM toroidal shell segments (TSSs) with porosities subjected to mechanical, thermal and thermomechanical loads. Results indicate that porosities have detrimental and beneficial influences on the buckling resistance of TSS under mechanical and thermal loads, respectively. The study is relatively general and has included an extensive region of tangential edge constraints and closed shell geometry.

2. The dissertation has suggested two-term form of deflection for the nonlinear stability analysis of FGM circular cylindrical shells with porosities and transverse shear deformation. The analysis suggests that for thick and moderately thick shells nonlinear axisymmetric term of deflection has marginal effect on the postbuckling behavior. Therefore, two-term deflection may be adequately accurate for the buckling and postbuckling analyses of shear deformable circular cylindrical shells.

3. The dissertation has analyzed the combined influences of porosities, tangential constraints of edges and three-parameter nonlinear elastic foundations on the nonlinear stability of FGM spherical caps under external pressure and circular plate under uniform temperature rise. The results of the dissertation reveal that FGM spherical caps being relatively shallow, with partially movable edges and resting on elastic foundation with suitable stiffnesses are the most stable because snapping jumps can be alleviated.

4. The dissertation has proposed a sandwich model with FG-CNTRC core and homogeneous face sheets. The results of dissertation find that, with the same volume percentage of material constituents, sandwich model constructed from thicker FG-CNTRC core along with stiff and thin homogeneous face sheets possesses many very advanced characteristics. This model may be standard sandwich structures due to high stiffness, be lightweight and good stability. The dissertation provides valuable suggestions for fabrication and application of sandwich structures made of FG-CNTRC.

LIST OF AUTHOR'S SCIENTIFIC WORKS RELATING TO THE CONTENT OF THE DISSERTATION

1. Vu Thanh Long and Hoang Van Tung, *Mechanical buckling analysis of thick FGM toroidal shell segments with porosities using Reddy's higher order shear deformation theory*, Mechanics of Advanced Materials and Structures. In Press. Published online: 24-8-2021. https://doi.org/10.1080/15376494.2021.1969606 (ISI, Q1).

2. Vu Thanh Long and Hoang Van Tung, *Buckling behavior of thick porous FGM toroidal shell segments under external pressure and elevated temperature including tangential edge restraint*, Journal of Pressure Vessel Technology, Transactions of the ASME, Vol. 144 (5), 2022, p. 051310 (11 pages). Published online: 11-1-2022. https://doi.org/10.1115/1.4053485 (ISI, Q2).

3. Vu Thanh Long and Hoang Van Tung, *Thermal nonlinear buckling of shear deformable functionally graded cylindrical shells with porosities*, AIAA Journal, Vol. 59 (6), 2021, pp. 2233-2241. https://doi.org/10.2514/1.J060026 (ISI, Q1)

4. Vu Thanh Long and Hoang Van Tung, *Thermomechanical nonlinear buckling of pressurized shear deformable FGM cylindrical shells including porosities and elastically restrained edges*, Journal of Aerospace Engineering, Transactions of the ASCE, Vol. 34 (3), 2021, p. 04021011 https://doi.org/10.1061/(ASCE)AS.1943-5525.0001252 (ISI, Q2).

5. Vu Thanh Long and Hoang Van Tung, *Postbuckling responses of porous FGM spherical caps and circular plates including edge constraints and nonlinear three-parameter elastic foundations*, Mechanics Based Design of Structures and Machines, 2021, pages 1-23. Article in Press. Published online: 2-8-2021. https://doi.org/10.1080/15397734.2021.1956327 (ISI, Q1).

6. Hoang Van Tung and Vu Thanh Long, *Buckling and postbuckling of CNT-reinforced composite sandwich cylindrical panels subjected to axial compression in thermal environments*, Vietnam Journal of Mechanics, VAST, Vol. 41 (3), 2019, pp. 217-231. https://doi.org/10.15625/0866-7136/13673.

7. Hoang Van Tung, Dao Nhu Mai and Vu Thanh Long, *Nonlinear response of doubly curved sandwich panels with CNT-reinforced composite core and elastically restrained edges subjected to external pressure in thermal environments*, Vietnam Journal of Mechanics, VAST, Vol. 44, No. 1, 2022, pp. 15-28. Published online: 11-12-2021. https://doi.org/10.15625/0866-7136/16575

8. Vu Thanh Long and Hoang Van Tung, *Thermal postbuckling behavior of CNT-reinforced composite sandwich plate models resting on elastic foundations with tangentially restrained edges and temperature-dependent properties*, Journal of Thermoplastic Composite Materials, Vol. 33 (10), 2020, pp. 1396-1428. https://doi.org/10.1177/0892705719828789 (ISI, Q2).

9. Vu Thanh Long and Hoang Van Tung, *Thermomechanical postbuckling behavior of CNT-reinforced composite sandwich plate models resting on elastic foundations with elastically restrained unloaded edges*, Journal of Thermal Stresses, Vol. 42 (5), 2019, pp. 658-680. https://doi.org/10.1080/01495739.2019.1571972 (ISI, Q1).